Neurosurg Rev (2013) 36:437–445
DOI 10.1007/s10143-013-0450-5

ORIGINAL ARTICLE

Differences between middle cerebral artery bifurcations with normal anatomy and those with aneurysms

Takashi Sadatomo · Kiyoshi Yuki · Keisuke Migita · Yasutaka Imada · Masashi Kuwabara · Kaoru Kurisu

Received: 26 February 2012 / Revised: 5 October 2012 / Accepted: 24 November 2012 / Published online: 26 January 2013

Abstract The objectives of this study were to elucidate the normal anatomy of middle cerebral artery (MCA) bifurcations and to analyze the differences in patients with MCA aneurysms. In the present study, 62 patients underwent three-dimensional magnetic resonance angiography, and no intracranial lesions were noted. The widths of M1 and the superior and inferior M2 branches, as well as their respective lateral angles, were measured. These values were used to calculate the daughter artery ratio (DA ratio; width of larger M2/width of smaller M2) and the lateral angle ratio (LA ratio; lateral angle between M1 and larger M2/lateral angle between M1 and smaller M2). The DA and LA ratios of 54 MCA aneurysm patients (34 with ruptured aneurysms, 20 with unruptured aneurysms) were also calculated, using three-dimensional digital subtraction angiography, and compared with the normal values. In normal patients, the widths of M1 and the branches of M2, the lateral angles, and the LA and DA ratios were not significantly different between the right and left sides. The bilateral superior and inferior lateral angles of normal MCAs were significantly wider than those of MCAs with aneurysms. The DA ratio was 1.5±0.4 in normal MCAs and 1.7±0.7 in MCAs with aneurysms; this difference was significant ($p<0.05$). The LA ratio was 1.3±0.4 in normal MCAs and 2.1±1.4 in MCAs with aneurysms; these values were also significantly different ($p<0.01$). Normal cerebral artery bifurcations show close to symmetric structure in the M2 branches and the lateral angles, whereas aneurysmal MCAs do not show this symmetry.

T. Sadatomo (✉) · K. Yuki · K. Migita · Y. Imada · M. Kuwabara
Department of Neurosurgery, Higashihiroshima Medical Center, Jike 513, Saijyo, Higashihiroshima, Hiroshima 739-0041, Japan
e-mail: sadatomo@k2.dion.ne.jp

K. Kurisu
Department of Neurosurgery, Graduate School of Biomedical and Health Sciences, Hiroshima University, Hiroshima, Japan

Keywords MCA · Anatomy · Aneurysm · 3D-MRA · 3D-DSA

Introduction

Many intracranial aneurysms occur at arterial bifurcations, and hemodynamic stress on these bifurcations is a mechanism of aneurysmal formation [20, 21]. In previous studies, we evaluated the relationship between aneurysmal neck location, daughter artery size, and lateral angles and reported that in many unruptured middle cerebral aneurysms, the aneurysmal necks deviate to the smaller daughter artery side [15–17]. In ruptured middle cerebral artery (MCA) aneurysms, the necks tend to be located on the midline of the bifurcation. Three-dimensional structures surrounding cerebral artery bifurcations vary with individual patients, including within the population of normal patients. There are currently no studies comparing these structures between patients with normal MCA bifurcations and those with bifurcations harboring MCA aneurysms. Our study is focused on analyzing the three-dimensional differences in these two types of MCA bifurcations. This type of structural study may provide clues for determining the morphological factors contributing to the development of aneurysms.

Patients and methods

Patient population

Magnetic resonance angiography (MRA) performed in 62 cases at the Higashihiroshima Medical Center did not reveal any vascular lesions. The middle cerebral artery (MCA) type included in this study was exclusively the bifurcation type, and trifurcation types were excluded. Thirty-five male and 27 female patients with ages ranging from 20 to 81

(mean; 59.4) were selected. The chief complaints were as follows: 18 cases of vertigo or dizziness, 9 of headache, 8 of numbness, 6 of tinnitus, 5 of facial palsy, 3 of brain check-up, 2 of visual field defect, and 1 each of sarcoidosis, trochlear nerve palsy, head injury, exophthalmos, eye-lid swelling, aortic valve stenosis, meningitis, ventricle dilatation, examination before coronary artery bypass grafting, and drug intoxication. There were four cases of trifurcation in the right MCA and five in the left MCA. These nine trifurcations were excluded from the study. The bifurcation point in this study was defined to be the ones that were the nearest from M1/M2 transition points and the bifurcating points of early branches are not included in this study. Thus, the anatomy of a total of 115 MCA bifurcations was examined.

Fifty-one consecutive patients with MCA aneurysm of the saccular type were hospitalized at the Higashihiroshima Medical Center, and three-dimensional digital subtraction angiography (3D-DSA) was performed in all of these patients. They included 19 male and 32 female patients, with ages ranging from 35 to 90 (mean; 61.3). The total number of aneurysms was 54, of which 34 aneurysms were ruptured (dome size; 6.7±3.2 mm) and 20 were unruptured (dome size; 5.6±3.5 mm). The age of cases with unruptured aneurysms was 61.2±14.6 and that with ruptured aneurysms was 61.4±7.3. They did not show statistically difference. In ruptured aneurysms, DSA studies were performed within 24 h from the onset in all cases.

3D-MRA and 3D-DSA studies

The Achieva 1.5-T Pulsar (Royal Philips Electronics, the Netherlands) was used for the MRA studies, and the Toshiba Infinix Celeve VC system (Toshiba, Inc., Tokyo, Japan) was used for the DSA studies. The raw data were transferred to the ZIO M900 workstation (Zio Software Inc., Tokyo, Japan) and analyzed to obtain the 3D information. The ZIO M900 workstation makes it possible to observe the MCA bifurcation with or without aneurysms from various angles and to measure the length, width, and the 3D angles of the arteries which constitute the MCA bifurcations.

Normal anatomy of the MCA bifurcations and anatomy of the MCA bifurcations with aneurysms

There are two lateral angles in each MCA bifurcation, which are situated between M1 and one of the M2 branches. The lateral angle between M1 and the superior M2 branch was called the superior lateral angle and that between M1 and the inferior M2 branch was called the inferior lateral angle. These two lateral angles were determined by viewing the plane decided by M1 and one of the M2 branches from the perpendicular direction (Fig. 1). In MCA aneurysm cases,

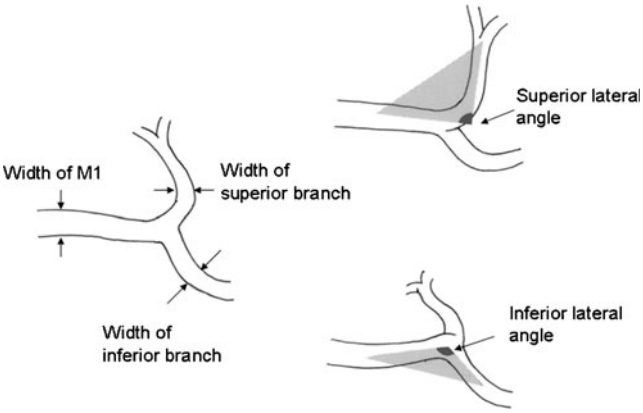

Fig. 1 *Shaded triangles* are planes described by M1 and either the superior or inferior M2 branches. *Upper right* superior lateral angle; *lower right* inferior lateral angle. The Zio M900 workstation automatically measures these angles when the examiner specifies the plane including M1 and 1 of the M2 branches

M1 is often called the parent artery and M2 is called the daughter artery. Whether the superior or the inferior branch of the M2 is larger is undecided, and it varies depending on individual cases. In this study, the daughter artery ratio (DA ratio) and lateral angle ratio (LA ratio) are defined as follows: DA ratio, width of larger M2 branch/width of smaller M2 branch and LA ratio, lateral angle between M1 and the larger M2 branch/lateral angle between M1 and the smaller M2 branch. When the widths of the two M2 branches are identical and the two lateral angles are not identical simultaneously, LA ratios are calculated as the larger lateral angle/smaller lateral angle.

The widths of the M1 and superior and inferior M2 branches, the superior and inferior lateral angles, and the DA and LA ratios were measured in normal MCA bifurcations using 3D-MRA and the ZIO M900 system. On the other hand, the superior and inferior lateral angles and the DA and LA ratios were measured using 3D-DSA and the ZIO M900 system for three categories, total aneurysm cases (both unruptured and ruptured aneurysm cases), unruptured aneurysm cases, and ruptured aneurysm cases. All these

Table 1 Measurement of normal MCA bifurcation

	Right	Left	*p* value
Width of M1 (mm)	2.2±0.3	2.2±0.2	0.2508
Width of superior branch (mm)	1.4±0.4	1.4±0.4	0.7352
Width of inferior branch (mm)	1.5±0.4	1.5±0.3	0.5867
Superior lateral angle (°)	117.1±22.1	119.7±24.3	0.5441
Inferior lateral angle (°)	107.2±24.9	113.5±25.9	0.1856
LA ratio	1.3±0.5	1.3±0.4	0.7866
DA ratio	1.5±0.4	1.4±0.4	0.2163

Table 2 Lateral angles of the normal MCA bifurcations

	Superior lateral angle	Inferior lateral angle	*p* value
Right (°)	117.1±22.1	107.2±24.9	0.0256
Left (°)	119.7±24.3	113.5±25.9	0.1948

data were statistically examined using Student's *t* test, which was performed using commercially available software (Stat View, version 5.0; SAS Institute, Inc., Cary, NC, USA).

Receiver operating characteristic analysis of lateral angles and LA and DA ratios

A receiver operating characteristic (ROC) analysis was performed to differentiate the lateral angles and the LA and DA ratios between the normal MCAs and the MCAs with aneurysms (including the three categories of total, unruptured, and ruptured aneurysm cases) and to differentiate LA and DA ratios between ruptured and unruptured aneurysms cases. The ROC analysis is commonly used when evaluating diagnostic tests [12]; the ROC curve is used to plot sensitivity against 1-specificity because the cutoff point varies continuously from larger to smaller values. Thus, for larger values of the cutoff point, sensitivity is low but specificity is high. As the cutoff point progressively decreases, sensitivity increases and specificity decreases. Thus, the curve is used to plot the trade-off between sensitivity and specificity, and the closer the curve is to the upper left-hand corner of the plot, the better the discrimination. The cutoff point was determined at the point where the Youden Index [3] shows the maximum value (Youden Index=sensitivity+specificity−1). Statistical Package for the Social Sciences (SPSS) II (SPSS Japan Inc., Tokyo, Japan) was used for the ROC analysis.

Results

Width of M1 and branches of M2, superior and inferior lateral angles, and LA and DA ratios in normal MCA bifurcations

The width of the right M1 was 2.2±0.3 mm and that of the left M1 was 2.2±0.2 mm. The width of the superior branch of the right M2 was 1.4±0.4 mm and that of the left M2 was 1.4±0.4 mm. The width of the inferior branch of the right M2 was 1.5±0.4 and that of the left M2 was 1.5±0.3 mm. The right superior lateral angle was 117.1±22.1°, and the left superior lateral angle was 119.7±24.3°. The right inferior lateral angle was 107.2±24.9°, and the left inferior lateral angle was 113.5±25.9°. Thus, the right LA ratio was 1.3±0.5, and the left LA ratio was 1.3±0.4. The right DA ratio was 1.5±0.4, and the left DA ratio was 1.4±0.4.

When the above values were compared between the right and left sides, they were not statistically different (Table 1). However, when the superior and inferior lateral angles were compared, the superior lateral angle was statistically wider than the inferior lateral angle on the right side ($p<0.05$). The superior lateral angle tended to be wider than the inferior lateral angle, but was not statistically different on the left side (Table 2).

Lateral angles of normal MCAs and MCAs with aneurysms

Four lateral angles were measured in this study: right superior, left superior, right inferior, and left inferior lateral angles. When these lateral angles were compared among normal MCA and total aneurysm cases (this category includes both ruptured and unruptured aneurysm cases), all of the four lateral angles were statistically wider in the normal MCA than those in the total aneurysm cases. When these lateral angles

Table 3 Lateral angles of the normal MCA and MCA with aneurysm

	Normal MCA	Total AN	*p* value
Right superior lateral angle (°)	117.1±22.1	92.3±33.6	<0.0001
Left superior lateral angle (°)	119.7±24.3	93.1±32.5	0.0002
Right inferior lateral angle (°)	107.2±24.9	93.2±38.3	0.0382
Left inferior lateral angle (°)	113.5±25.9	84.2±46.7	0.0008
	Normal MCA	Unruptured AN	*p* value
Right superior lateral angle (°)	117.1±22.1	83.2±37.3	<0.0001
Left superior lateral angle (°)	119.7±24.3	91.3±37.4	0.0081
Right inferior lateral angle (°)	107.2±24.9	96.1±45.7	0.2255
Left inferior lateral angle (°)	113.5±25.9	68.6±42.8	0.0002
	Normal MCA	Ruptured AN	*p* value
Right superior lateral angle (°)	117.1±22.1	97.1±31.0	0.0029
Left superior lateral angle (°)	119.7±24.3	93.9±31.2	0.0013
Right inferior lateral angle (°)	107.2±24.9	91.4±33.9	0.0292
Left inferior lateral angle (°)	113.5±25.9	92.1±48.0	0.0251

Table 4 Daughter artery ratio and lateral angle ratio

	Normal MCA	Total AN	*p* value	Cut point
DA ratio	1.5±0.4	1.7±0.7	0.0193	–[a]
LA ratio	1.3±0.4	2.2±1.4	<0.0001	1.6
	Normal MCA	Unruptured AN	*p* value	Cut point
DA ratio	1.5±0.4	2.1±0.8	<0.0001	1.9
LA ratio	1.3±0.4	2.6±1.4	<0.0001	1.6
	Normal MCA	Ruptured AN	*p* value	Cut point
DA ratio	1.5±0.4	1.4±0.5	0.6033	–[a]
LA ratio	1.3±0.4	1.9±1.3	<0.0001	1.6
	Ruptured AN	Unruptured AN	*p* value	Cut point
DA ratio	1.4±0.5	2.1±0.8	0.0001	1.7
LA ratio	1.9±1.3	2.6±1.4	0.07	–[a]

[a]Cut point did not detected because it did not reach significant differences by ROC analysis

were compared among normal MCA and ruptured aneurysm cases, all of the four lateral angles were also statistically wider in the normal MCA than those in the ruptured aneurysm cases. When these lateral angles were compared among normal MCA and unruptured aneurysm cases, three of the four lateral angles were statistically wider in the normal MCA than those in the unruptured aneurysm cases (Table 3).

DA and LA ratios of normal MCA and MCA aneurysm cases

The DA ratio of the normal MCA cases, which includes both left and right sides, was 1.5±0.4 and that of the total aneurysm cases, which includes both ruptured and unruptured aneurysm cases, was 1.7±0.7. A significant difference was calculated ($p<0.05$) using Student's *t* test. When the DA ratios of normal MCA and unruptured aneurysm cases (DA ratio=2.1±0.8) were compared, the difference was more prominent ($p<0.01$). On the contrary, when the DA rations of normal MCA and ruptured aneurysm cases (1.4±0.5) were compared, no statistically significant differences were observed. The LA ratio of the normal MCA cases was 1.3±0.4 and that of the total aneurysm cases was 2.2±1.4, which demonstrated a significant difference ($p<0.01$) using Student's *t* test. The LA ratio in both the unruptured (2.6±1.4) and ruptured (1.9±1.3) aneurysm cases demonstrated a

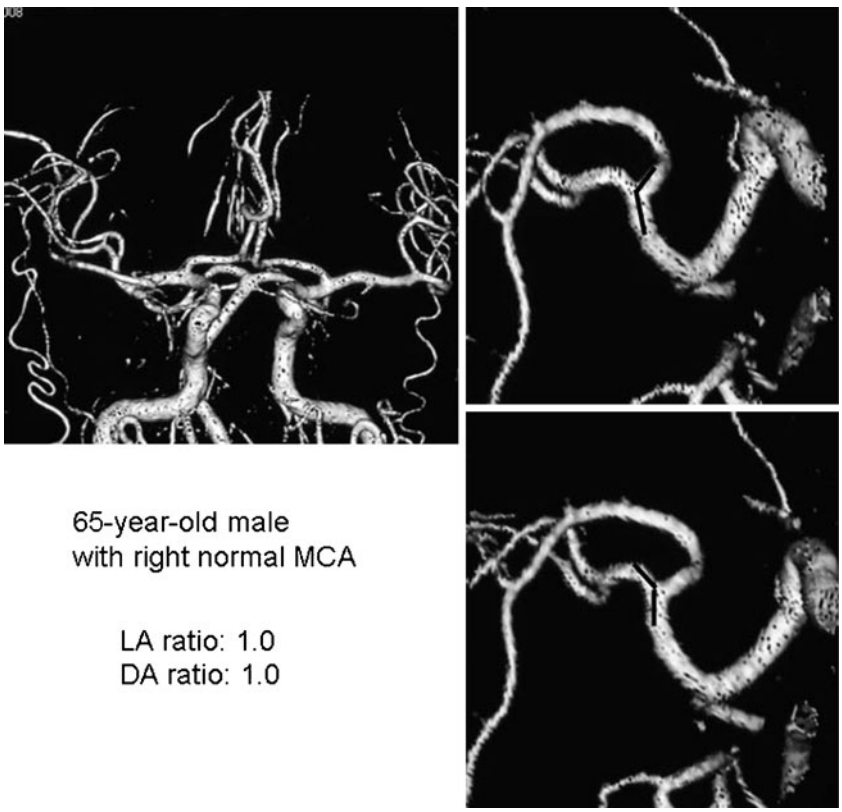

Fig. 2 Representative normal right middle cerebral artery (*MCA*) in a 65-year-old man. The superior lateral and inferior lateral angle measures as well as their widths are almost the same. Thus, both the lateral angle (*LA*) and daughter artery (*DA*) ratios are 1.0

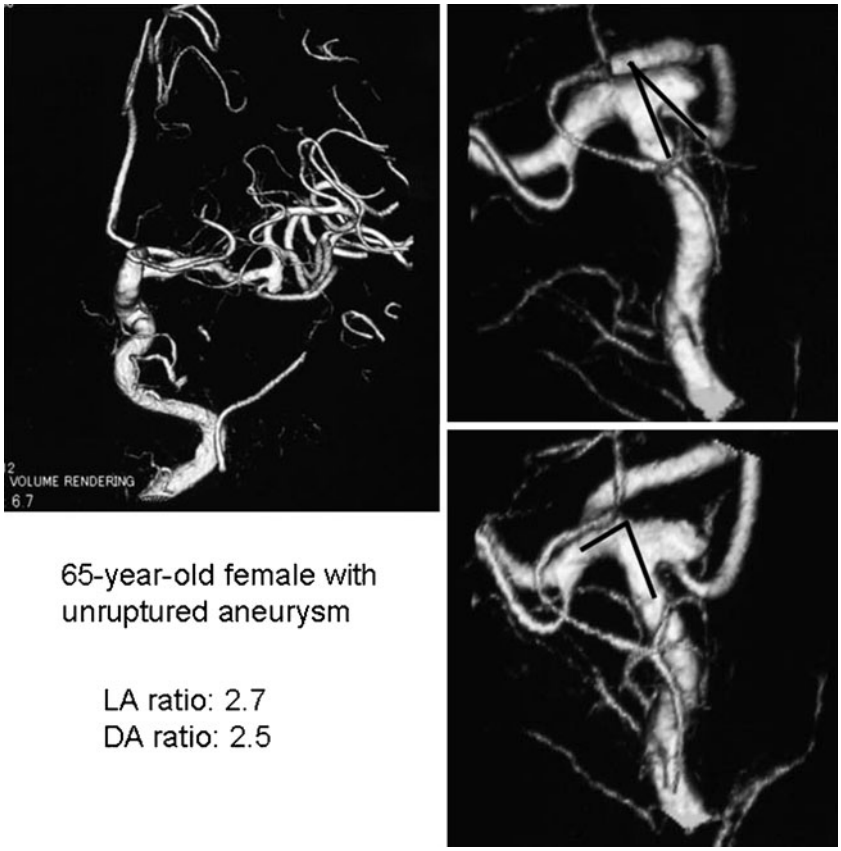

Fig. 3 Representative left MCA unruptured aneurysm in a 65-year-old woman. Both the LA and DA ratios are high, at 2.7 and 2.5, respectively

significantly high count compared to the normal MCA cases (both of them $p<0.01$) (Table 4). Representative cases of normal MCA, MCA with unruptured and ruptured aneurysm are shown in Figs. 2, 3, and 4 respectively.

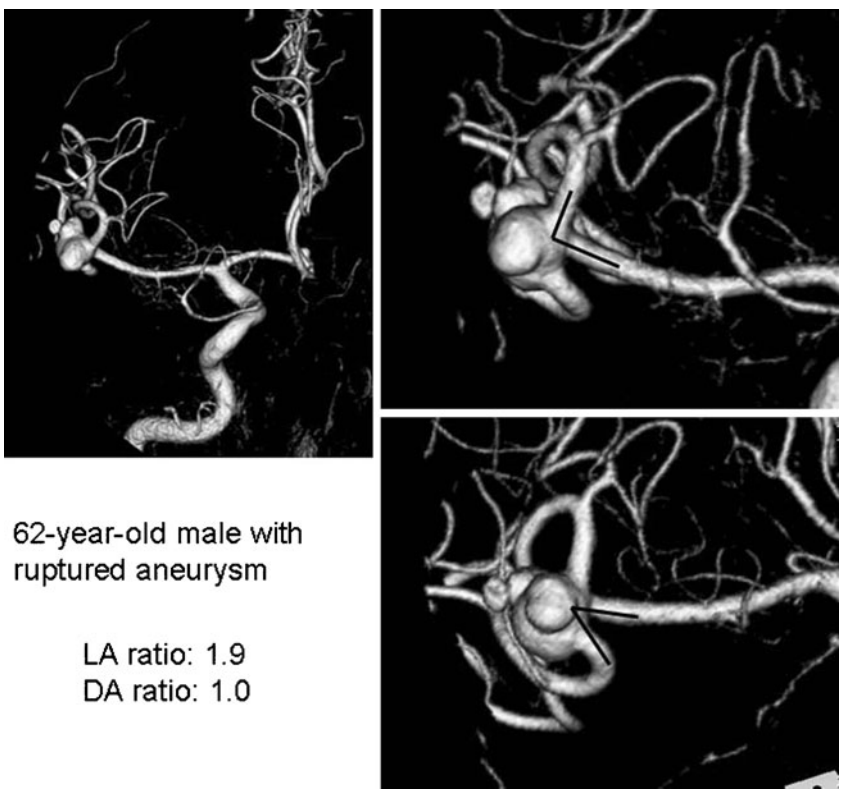

Fig. 4 Representative right MCA ruptured aneurysm in a 62-year-old man. The LA ratio is high, at 1.9. However, the DA ratio is low, at 1.0

Receiver operating characteristic analysis on lateral angles, and LA and DA ratios

Student's *t* test revealed that there was a significant difference between the DA ratios of the normal MCA and total aneurysm cases. However, no significant difference was observed on ROC analysis. The LA ratios of the normal MCA and total aneurysm cases, both the DA and LA ratios of the normal MCA and unruptured aneurysm cases, the LA ratio of the normal MCA and ruptured aneurysm cases, and the DA ratio of the ruptured and unruptured aneurysm cases demonstrated significant differences by ROC analysis, and their cut-off points were 1.6, 1.9, 1.6, and 1.7, respectively (Table 4). The ROC curves of the two representatives are shown in Fig. 5.

Discussion

With the advent of 3D-DSA and 3D time-of-flight MRA, it has become possible to obtain detailed information regarding the cerebral arteries [1, 5, 8, 9, 14]. Morphological evaluation of the circle of Willis in healthy patients using DSA and MRA is currently under-reported [10, 22], and extensive studies have not been performed.

The width of M1 and the branches of M2, as measured in healthy Japanese patients by MRA, were approximately 2.2 and 1.4–1.5 mm, respectively, in our study. In a previous report from Poland, the widths of M1 and the branches of M2, measured by MRA, were approximately 2.4 and 1.6–1.7 mm, respectively [22]. These slight differences may be due to variable imaging conditions during MRA, or due to racial differences. The average width of M1 in a cadaveric brain has been reported as 3.9 mm [6], which was quite different from our results. However, the width of M1 in the cadaveric brain was obtained by measuring the outside diameter, whereas we measured the inside diameter to obtain our result; this may be the main reason for the discrepancy. In addition, the MRA value represents the flow inside the artery, which tends to be narrower than the actual inside diameter.

In this study, superior and inferior lateral MCA angles were measured. The former tended to be wider than the latter on the left side, and this difference reached statistical significance on the right side. When LA ratios were calculated; however, no significant differences in the extent of lateral angle asymmetry were observed between the right and left sides. When lateral angles were compared between normal MCAs and the MCAs of aneurysm patients, the four lateral angles (right superior, left superior, right inferior, and left inferior) in the aneurysm cases were significantly smaller than those in the normal patients. This may be because aneurysms are space-occupying lesions that dislocate the M2 branches to the lateral side; thus, the lateral angles became smaller. Even if no other reason exists, by this argument, the lateral angles of MCAs with ruptured

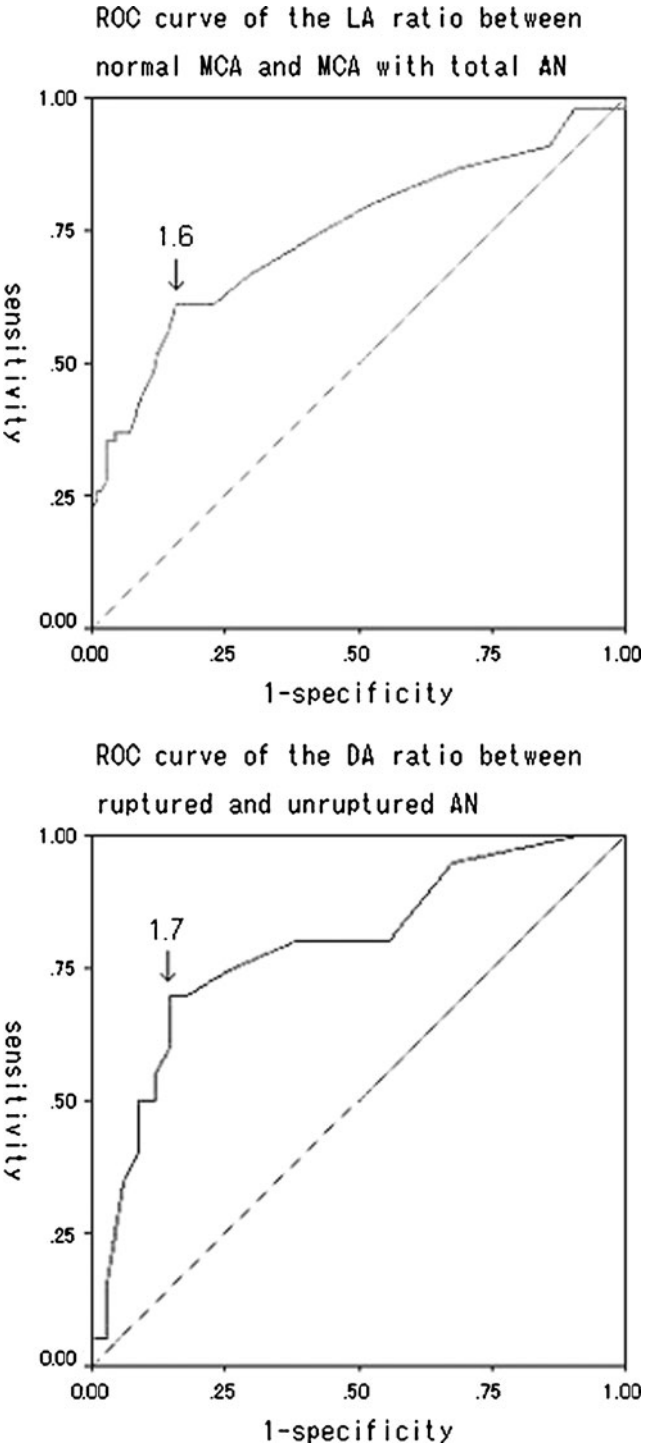

Fig. 5 *Top* The area under the receiver operating characteristic (*ROC*) curve for the LA ratio between normal MCAs and all MCAs with aneurysm is 0.74 [95 % confidence interval (CI), 0.66–0.83]. The cutoff point for the LA ratio is 1.6, the sensitivity is approximately 61 %, and the specificity is 84 %. *Bottom* The area under the ROC curve for the DA ratio between ruptured and unruptured aneurysmal vessels is 0.79 (95 % CI, 0.66–0.92). The cutoff point for the LA ratio is 1.6, the sensitivity is approximately 70 %, and the specificity is 85 %

aneurysms would be smaller than those with unruptured aneurysms, as ruptured aneurysms are larger than their unruptured counterparts (as mentioned in the "Patients and methods" section). A comparison of the lateral angles, calculated as the average of the superior and inferior lateral angles, yielded different results. The average value of the lateral angles of right MCAs with ruptured aneurysms was 188.5°, whereas that of right MCAs with unruptured aneurysms measured 179.3°. The average value of the lateral angles of left MCAs with ruptured aneurysms was 186.0°, whereas that of the left MCAs with unruptured aneurysms measured 159.9°. The average value of the lateral angles of MCAs with ruptured aneurysms was larger, not smaller, than that of their unruptured counterparts. Therefore, another factor besides space occupation may be responsible for the differences in lateral angle measurements in MCAs with aneurysms.

The possibility that a smaller lateral angle per se is the structural cause of a developing aneurysm cannot be ruled out. To clarify this, it is necessary to compare the same patient's bifurcations by 3D-MRA or 3D-DSA before and after aneurysmal development. In our series, there was only one example of such a comparison. A 72-year-old male was referred to our hospital for an incidentally discovered unruptured aneurysm. He had been evaluated 11 years ago by MRA in another hospital; however, as three-dimensional images were not available from this study, the precise lateral angles could not be measured. There were, however, no conspicuous differences in the construction of the parent and daughter arteries when comparing images obtained after aneurysmal development to the baseline images (Fig. 6). If it is confirmed that lateral MCA angles do not show significant changes before and after aneurysmal development, a smaller lateral angle or development of asymmetry in the lateral angles could be considered as risk factors for future aneurysmal formation.

The Student's *t* test demonstrated that the DA and LA ratios of normal MCAs were both significantly smaller than those of MCAs with aneurysms. However, when they were compared by ROC analysis, significant differences were observed only for the LA ratios; the cutoff point was 1.6. These results mimicked those of the comparison between normal MCAs and MCAs with ruptured aneurysms. However, the DA and LA ratios of MCAs with unruptured aneurysms both indicated a significant difference by ROC analysis when compared with normal MCAs. Thus, the lateral angle of MCAs with aneurysms, regardless of whether they are ruptured or unruptured, tends to be asymmetrical. However, an asymmetrical M2 width is a feature specific to MCAs with unruptured aneurysms. The DA ratio of unruptured aneurysms is significantly higher than that of ruptured aneurysms, with a cutoff point of 1.7. This result is consistent with that of our previous report [17].

This retrospective study aims to clarify the morphological differences between normal vessels and vessels containing aneurysms. In ruptured aneurysms, the influences of hematoma, vasospasm, brain edema, and hydrocephalus on the measurement of the lateral angles and the width of daughter arteries must be considered. In our series, there were no cases of massive hematoma, and DSA was performed within 24 h of the onset of symptoms. Therefore, the influence of the first two factors can be ignored. However,

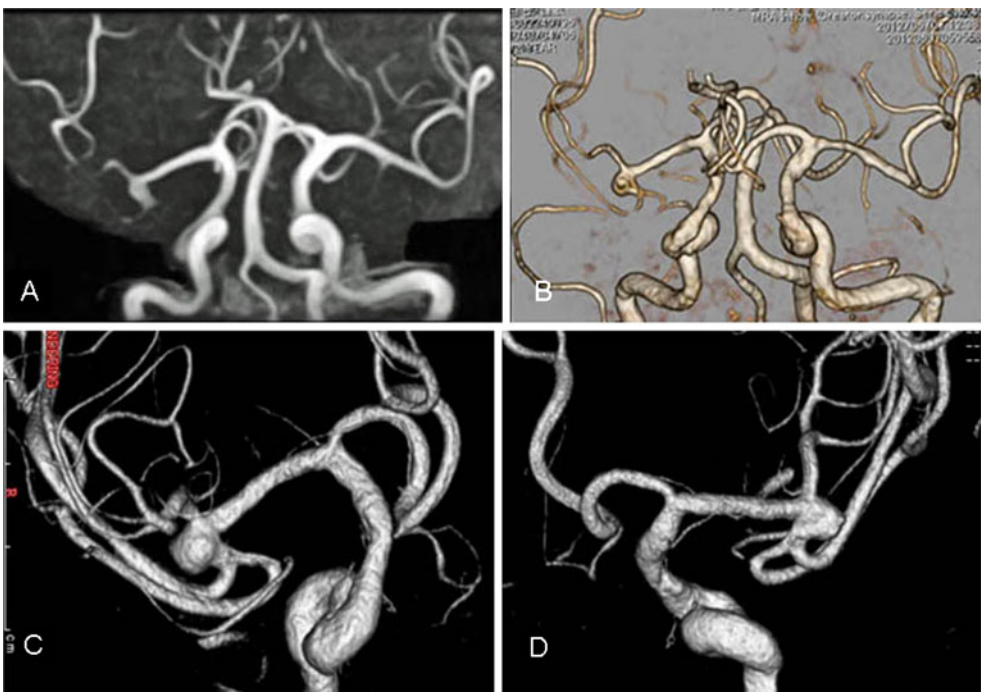

Fig. 6 A case of unruptured aneurysm. A 72-year-old male had been evaluated 11 years ago by MRA in another hospital (**a**) although three-dimensional images were not available from this study. The precise lateral angles could not be measured. There were, however, no conspicuous differences in the construction of the parent and daughter arteries when comparing images of the MRA obtained after aneurysmal development (**b**) to the baseline images. **c**, **d** The three-dimensional DSA of the same patient

the influence of the latter two cannot be ruled out. A prospective study focusing on these morphological points may help to clarify the characteristics that predict aneurysmal development or rupture; this is very useful information for those without aneurysms or who have unruptured aneurysms.

Reports describing computational flow dynamic studies on aneurysms per se or on parent arteries are gradually increasing [7, 13, 23–25]. There is a particular focus on wall shear stress as a possible mechanism of aneurysmal formation. It has been reported that high wall shear stress plays an important role in aneurysm initiation and growth [4, 11]. However, Shojima et al. [18, 19] and Doenitz et al. [2] proposed that reducing wall shear stress inside an aneurysm leads to its progression and eventual rupture. Flow dynamic studies focusing on the structural differences in the daughter arteries, including normal cerebral artery bifurcations, have not been adequately performed. These studies would be useful in understanding the mechanism of aneurysm formation and rupture.

In conclusion, we found that MCA bifurcations in patients with aneurysms show differences from their normal counterparts. The lateral angles are more narrow in patients with aneurysms, and the angles in bifurcations with aneurysms tend to be asymmetrical. Unruptured aneurysms tend to have asymmetrical widths of M1 and M2. Prospective studies concerning these characteristics may help clinicians to predict which currently normal MCAs are prone to future aneurysm or rupture.

References

1. Deutschmann HA, Augustin M, Simbrunner J, Unger B, Schoellnast H, Fritz GA, Klein GE (2007) Diagnostic accuracy of 3D time-of-flight MR angiography compared with digital subtraction angiography for follow-up of coiled intracranial aneurysms: influence of aneurysm size. AJNR Am J Neuroradiol 28(4):628–634
2. Doenitz C, Schebesch KM, Zoephel R, Brawanski A (2010) A mechanism for the rapid development of intracranial aneurysms: a case study. Neurosurgery 67(5):1213–1221
3. Fluss R, Faraggi D, Reiser B (2005) Estimation of the Youden Index and its associated cutoff point. Biom J 47(4):458–472
4. Foutrakis GN, Yonas H, Sclabassi RJ (1999) Saccular aneurysm formation in curved and bifurcating arteries. AJNR Am J Neuroradiol 20(7):1309–1317
5. Gauvrit JY, Leclerc X, Vermandel M, Lubicz B, Despretz D, Lejeune JP, Rousseau J, Pruvo JP (2005) 3D rotational angiography: use of propeller rotation for the evaluation of intracranial aneurysms. AJNR Am J Neuroradiol 26(1):163–165
6. Gibo H, Carver CC, Rhoton AL Jr, Lenkey C, Mitchell RJ (1981) Microsurgical anatomy of the middle cerebral artery. J Neurosurg 54(2):151–169
7. Hassan T, Hassan AA, Ahmed YM (2011) Influence of parent vessel dominancy on fluid dynamics of anterior communicating artery aneurysms. Acta Neurochir (Wien) 153(2):305–310
8. Hirai T, Korogi Y, Suginohara K, Ono K, Nishi T, Uemura S, Yamura M, Yamashita Y (2003) Clinical usefulness of unsubtracted 3D digital angiography compared with rotational digital angiography in the pretreatment evaluation of intracranial aneurysms. AJNR Am J Neuroradiol 24(6):1067–1074
9. Kang HS, Han MH, Kwon BJ, Jung SI, Oh CW, Han DH, Chang KH (2004) Postoperative 3D angiography in intracranial aneurysms. AJNR Am J Neuroradiol 25(9):1463–1469
10. Krabbe-Hartkamp MJ, van der Grond J, de Leeuw FE, de Groot JC, Algra A, Hillen B, Breteler MM, Mali WP (1998) Circle of Willis: morphologic variation on three-dimensional time-of-flight MR angiograms. Radiology 207(1):103–111
11. Meng H, Wang Z, Hoi Y, Gao L, Metaxa E, Swartz DD, Kolega J (2007) Complex hemodynamics at the apex of an arterial bifurcation induces vascular remodeling resembling cerebral aneurysm initiation. Stroke 38(6):1924–1931
12. Metz CE (1978) Basic principles of ROC analysis. Semin Nucl Med 8:283–298
13. Ohshima T, Miyachi S, Hattori K, Takahashi I, Ishii K, Izumi T, Yoshida J (2008) Risk of aneurysmal rupture: the importance of neck orifice positioning-assessment using computational flow simulation. Neurosurgery 62(4):767–773, discussion 773–5
14. Piotin M, Gailloud P, Bidaut L, Mandai S, Muster M, Moret J, Rüfenacht DA (2003) CT angiography MR angiography and rotational digital subtraction angiography for volumetric assessment of intracranial aneurysms. An experimental study. Neuroradiology 45 (6):404–409
15. Sadatomo T, Yuki K, Migita K, Taniguchi E, Kodama Y, Kurisu K (2005) Evaluation of relation among aneurysmal neck, parent artery, and daughter arteries in middle cerebral artery aneurysms, by three-dimensional digital subtraction angiography. Neurosurg Rev 28(3):196–200
16. Sadatomo T, Yuki K, Migita K, Taniguchi E, Kodama Y, Kurisu K (2006) The characteristics of the anterior communicating artery aneurysm complex by three-dimensional digital subtraction angiography. Neurosurg Rev 29(3):201–207
17. Sadatomo T, Yuki K, Migita K, Taniguchi E, Kodama Y, Kurisu K (2008) Morphological differences between ruptured and unruptured cases in middle cerebral artery aneurysms. Neurosurgery 62 (3):602–609, discussion 602–9
18. Shojima M, Oshima M, Takagi K, Torii R, Hayakawa M, Katada K, Morita A, Kirino T (2004) Magnitude and role of wall shear stress on cerebral aneurysm: computational fluid dynamic study of 20 middle cerebral artery aneurysms. Stroke 35(11):2500–2505
19. Shojima M, Nemoto S, Morita A, Oshima M, Watanabe E, Saito N (2010) Role of shear stress in the blister formation of cerebral aneurysms. Neurosurgery 67(5):1268–1274
20. Stehbens WE (1989) Etiology of intracranial berry aneurysms. J Neurosurg 70:823–831
21. Steiger HJ (1990) Pathophysiology of development and rupture of cerebral aneurysms. Acta Neurochir Suppl (Wien) 48:1–57
22. Tarasów E, Abdulwahed Saleh Ali A, Lewszuk A, Walecki J (2007) Measurements of the middle cerebral artery in digital subtraction angiography and MR angiography. Med Sci Monit 13 (Suppl 1):65–72
23. Tateshima S, Chien A, Sayre J, Cebral J, Viñuela F (2010) The effect of aneurysm geometry on the intra-aneurysmal flow condition. Neuroradiology 52(12):1135–1141
24. Valen-Sendstad K, Mardal KA, Mortensen M, Reif BA, Langtangen HP (2011) Direct numerical simulation of transitional flow in a patient-specific intracranial aneurysm. J Biomech 44(16):2826–2832
25. Xiang J, Tremmel M, Kolega J, Levy EI, Natarajan SK, Meng H (2011) Newtonian viscosity model could overestimate wall shear stress in intracranial aneurysm domes and underestimate rupture risk. J Neurointerv Surg. doi:10.1136/neurintsurg-2011-010089

Comments

Waleed A. Azab, Safat, Kuwait

In this study, Sadatomo et al. utilized 3D-DSA in patients with MCA saccular aneurysms and MRA in normal subjects to analyze the morphometry of MCA bifurcations in patients with and without MCA aneurysmal rupture. They found that MCA bifurcations in patients with aneurysms show differences from their normal counterparts; the lateral angles are more narrow in patients with aneurysms, the angles in bifurcations with aneurysms tend to be asymmetrical, and unruptured aneurysms tend to have asymmetrical widths of M_1 and M_2.

Although factors other than vessel diameters and take off angles may be contributing to aneurysmal rupture and measurements could be compromised by vasospasm in patients with post-aneurysmal rupture SAH, the findings of the study add to our understanding of the mechanisms underlying MCA aneurysm rupture and can potentially help predicting such an event and treating it in a timely fashion.

Simone Peschillo and Roberto Delfini, Rome, Italy

In this interesting article by Sadatomo et al., the authors have studied 62 patients without vascular lesions and 51 consecutive patients with saccular aneurysms of the MCA in order to be able to compare, between the two patient populations, the size and the angles measured at the level of the MCA bifurcation. When these lateral angles were compared among normal MCA and total ruptured and unruptured aneurysm cases, all of the four lateral angles studied were statistically wider in the normal MCA than those in the total aneurysm cases. When these lateral angles were compared among normal MCA and ruptured aneurysm cases, all of the four lateral angles were also statistically wider in the normal MCA than those in the ruptured aneurysm cases. This is very interesting because of the potential useful information that could emerge from a neuroradiological study of the patient: In particular, a smaller lateral angle or development of asymmetry in the lateral angles could be considered as risk factors for future aneurysmal formation or rupture and, thus, address the patient to further controls. As mentioned by the Authors, a prospective study focusing on these morphological points may help to clarify the characteristics that predict aneurysmal development or rupture.

Hussam Metwali, Hannover, Germany

In this article, the authors studied the difference between the configuration of middle cerebral artery bifurcation in the presence and absence of aneurysm. This series includes ruptured and unruptured aneurysms. The influence of the presence of an aneurysm is studied in the terms of changes in the lateral angle ratio and the daughter artery ratio. Significant differences were found. Sadatomo et al. stated that this difference can help to understand the etiology of the formation of an aneurysm and mechanism of its rupture.

Although the clinical impact of this study is not clear, it can help with further flow dynamic studies to understand the flow stresses at the moment of study but in our eyes still cannot clarify the cause/result dilemma of aneurysmal development. It is difficult to say if this change is the cause of the aneurysmal development or it is a deformation due to the presence of an aneurysm. This may require the angiographies of the patients before development of the aneurysm to be studies in conjunction of the angiographies of the same patients after development of the aneurysm. We recommend the author to continue their work screening high-risk population and pick the population who will develop the disease.